T1−T1 Interactions Occur in ER Membranes while Nascent Kv Peptides Are Still Attached to Ribosomes†

Jianli Lu, John M. Robinson, David Edwards, and Carol Deutsch*

Department of Physiology, University of Pennsylvania, Philadelphia, Pennsylvania 19104-6085

Received April 16, 2001; Revised Manuscript Received July 13, 2001

ABSTRACT: For voltage-gated K^+ channels (Kv), it is not clear at which stage during biosynthesis in the endoplasmic reticulum (ER) oligomerization occurs, specifically whether it can begin while nascent peptide chains of individual subunits are still attached to ribosomes. Kv channels possess a T1-recognition domain in the NH_2-terminus, which confers subfamily specificity for intersubunit assembly and forms a tetramer. Using pairs of cysteines engineered into the T1−T1 interface and cross-linking methods, we show that specific residues in the T1−T1 interface of different Kv1.3 subunits come into close proximity in the ER, both in microsomal membranes and in *Xenopus* oocytes. Furthermore, using translocation intermediates containing pairs of engineered cysteines in the T1 interface, we demonstrate that specific residues in the folded T1 domain interface can approach within 2 Å of each other and form tetramers while the nascent Kv1.3 peptides are still attached to ribosomes and have translocated across the membrane. ER membranes are required for this interaction, and T1−T1 interactions occur inter-polysomally. Thus, folding of the T1 domain and intersubunit interaction may represent the first assembly event in channel formation.

Tetrameric voltage-gated potassium channels (Kv) originate as nascent monomeric peptides. The intervening sequence of events holds clues to the molecular mechanisms underlying channel formation, but unfortunately this sequence is not understood in detail. Conventional scenarios of these events suggest the following order: first, the monomeric protein is synthesized and integrated into the membrane, followed by oligomerization to form mature tetrameric structures, which then exit the endoplasmic reticulum (ER) and migrate to the plasma membrane. However, these processes could overlap in time or be coordinated or cooperative.

The first evidence that tetrameric channels form in the ER membrane came in 1992 from the work of Rosenberg and East (*1*), who showed that *Shaker* translated in vitro in microsomal membranes and reconstituted into bilayers produced functional channels. At about the same time, it was shown that Kv channels contain an N-terminal domain that is responsible for subfamily specific co-assembly of subunits (*2*). Moreover, for Kv1.1, Pfaffinger and co-workers reported that subunit−subunit interactions occurred in the ER, tetramers were held together by noncovalent interactions, and subunits lacking this N-terminal domain could not homomultimerize (*3*). This N-terminal region was thought to be a tetramerization domain and was therefore christened the "T1 domain" (*3*). None of these studies addressed the question of when during biogenesis tetramer formation occurs. The first implication came from the finding that Kv1.1 and Kv1.4, when translated together, form heteromultimers within 15 min of the start of translation in microsomal membranes (*4*). That is, at the earliest time that protein was detected, heteromers were formed, as determined by co-immunoprecipitation. However, the antibodies used in this study were directed at the C-terminus of the Kv proteins so that only fully synthesized protein was detected, thereby precluding resolution of the protein domains involved and of the timing of the oligomerization steps. The authors comment, however, "It is possible that assembly begins early in translation, perhaps via the interaction of N-terminal sequences as previously suggested by Li et al. (1992)". Although they conclude that heteromeric assembly is perhaps co-translational, their results only indicate that association is rapid and coincident with the appearance of protein, but do not exclude a series of rapid and nonoverlapping steps between synthesis and association.

Specific tetramer (vis-à-vis heteromer) formation in the ER in vivo was clearly shown for *Shaker* Kv channels by Nagaya and Papazian (*5*), but no temporal assignment was made. The same group demonstrated that tetramer formation in the ER requires T1, that folding of the voltage-sensor and pore formation require T1, that α and β subunit association requires T1 (also see refs *6* and *7*), and that prefolded monomers are not required for oligomerization (*8*). However, these findings do not demonstrate direct T1−T1 interactions in the ER. These authors place tetramerization after protein synthesis, glycosylation, and insertion into the membrane. This temporal assignment was not based on simultaneous measurement of the time course of these events, but rather on logical inference.

Two recent studies present evidence in support of a T1 tetrameric structure in the full-length, mature Kv channel in the plasma membrane (*9*, *10*). But when, in the ontogeny of Kv channels, is this structure formed? Is it already formed in the ER membrane and how early in biogenesis? For

† Supported by National Institutes of Health Grant GM 52302.

* Corresponding author: Carol Deutsch, Department of Physiology, University of Pennsylvania, Philadelphia, PA 19104-6085. Phone: 215-898-8014; fax: 215-573-5851; e-mail: cjd@mail.med.upenn.edu.

10.1021/bi010763e CCC: $20.00
Published on Web 08/21/2001

homooligomers, it might make sense to take advantage of the natural proximity of neighboring nascent peptide chains as they are being synthesized from nearby ribosomes on a polysome. To test whether Kv nascent peptides attached to ribosomes are close enough to interact with each other, we generated translocation intermediates that remain attached to ribosomes and used bifunctional cross-linkers or oxidizing agents to cross-link engineered pairs of cysteines at putative interaction sites in the folded T1−T1 interface of Kv1.3 channels. These sites are predicted by the crystal structure of the T1 domain (*11*−*13*) and have been experimentally tested by Miller and co-workers for mature *Shaker* channels expressed in oocytes (*9*). The region crystallized is virtually identical to the T1 region of Kv1.3, the Kv protein used in this study.

In this paper, we present evidence of early, close proximity between neighboring subunits while the nascent peptides are still attached to ribosomes and have translocated across the membrane, suggesting that tetramers can form prior to polypeptide exit from the ER translocation channel. Furthermore, this proximity is specific for residues in the folded T1 domain interface. Thus, folding of the T1 domain and intersubunit T1−T1 interaction may represent the first assembly event in channel formation.

METHODS AND MATERIALS

Recombinant DNA Techniques. Standard methods of plasmid DNA preparation, restriction enzyme analysis, agarose gel electrophoresis, and bacterial transformation were used. All isolated fragments were purified with "Geneclean" (Bio 101 Inc., La Jolla, CA), recircularized using T4 DNA ligase and then used to transform DH5α or JM 109 competent cells (Promega, Madison, WI). The nucleotide sequences of all mutants were confirmed by restriction enzyme analysis or by automated cycle sequencing performed by the DNA Sequencing Facility at the School of Medicine on an ABI 377 Sequencer using Big dye terminator chemistry (ABI).

Plasmid Constructs. All mutant DNAs were sequenced in the region of the mutation. Additionally, for cysteine-free and engineered R118C/D126C, R116C/E130C, and R62C/E64C, the entire open reading frame of the gene was sequenced. pSP/Kv1.3/cysteine-free was generated by stepwise removal of all 12 native cysteines from the pSP/Kv1.3 template using QuikChange site-directed mutagenesis kit (Stratagene, La Jolla, CA) and the relevant sense and antisense oligonucleotides. This procedure also generated constructs with intermediate numbers of cysteines. The mutations are in order from the first cysteine in the sequence (C1) to the last (C12): C26S, C31S, C49S, C50S, C71S, C200V, C250S, C265S, C412A, C453S, C504S, and C513S. pSP/Kv1.3/C1−C5$^+$/C6−C9$^-$/C10−C12$^+$ (referred to as C1−C5$^+$ in the text and figures when used in *BstEII*-cut translocation intermediates lacking the C-terminus) contained mutated C6−C9 (C200V, C250S, C265S and C412A). pSP/Kv1.3/C1−C4$^-$/C5$^+$/ C6−C9$^-$/C10−C12$^+$ (referred to as C5$^+$ in the text and figures when used in *BstEII*-cut translocation intermediates lacking the C-terminus) contained mutated C1−C4 (C26S, C31S, C49S and C50S) as well as mutated C6−C9 (C200V, C250S, C265S and C412A). pSP/Kv1.3/C1−C2$^-$/C3−C5$^+$/ C6−C9$^-$/C10−C12$^+$ (referred to as C3−C5$^+$ in the text and figures when used in *BstEII*-cut translocation intermediates lacking the C-terminus) contained mutated C1−C2 (C26S and C31S) as well as mutated C6−C9 (C200V, C250S, C265S and C412A). pSP/Kv1.3/ C1$^+$-C2$^+$/C3−C4$^-$/C5$^+$/ C6−C9$^-$/C10−C12$^+$ (referred to as C1/C2/C5$^+$ in the text and figures when used in *BstEII*-cut translocation intermediates lacking the C-terminus) contained mutated C3−C4 (C49S and C50S) as well as mutated C6−C9 (C200V, C250S, C265S, and C412A). pSP/Kv1.3/C1−C9$^-$/C10−C12$^+$ (referred to as Cys-free in the text and figures when used in *BstEII*-cut translocation intermediates lacking the C-terminus) contained mutated C1−C5 (C26S, C31S, C49S, C50S, and C71S) as well as mutated C6−C9 (C200V, C250S, C265S, and C412A). Engineered cysteines were also introduced using QuikChange site-directed mutagenesis kit. pSP/Kv1.3/ C1−C10$^-$/C11−C12$^+$/ R118C/D126C is referred to as R118C/D126C in the text and figures when used in *KpnI*-, *BstEII*-, or *AfeI*-cut translocation intermediates lacking the C-terminus. pSP/Kv1.3/ C1−C9$^-$/C10−C12$^+$/ R116C/E130C is referred to as R116C/E130C in the text and figures when used in *BstEII*-cut translocation intermediates lacking the C-terminus. pSP/Kv1.3/ C1−C9$^-$/C10−C12$^+$/ R62C/E64C is referred to as R62C/E64C in the text and figures when used in *BstEII*-cut translocation intermediates lacking the C-terminus. pSP/Kv1.3/C1−C5$^-$/C6−C9$^+$/C10−C12$^-$/R118C/D126C/Flag, pSP/Kv1.3/C1−C5$^-$/ C6−C9$^+$/C10−C12$^-$/ R116C/E130C/Flag, and pSP/Kv1.3/C1−C5$^-$/C6−C9$^+$/C10−C12$^-$/ R62C/E64C/Flag are referred to as full-length R116C/D126C, R118/E130C, and R62C/E64C in the text and figures. They were generated from a pSP/Kv1.3/Flag template.

In Vitro Translation. Capped cRNA was synthesized in vitro from linearized templates using Sp6 RNA polymerase (Promega, Madison, WI). Full-length Kv1.3 linearized template was generated using *EcoRI* enzyme digestion; linearized templates for Kv1.3 translocation intermediates were generated using *BstEII*, *KpnI*, or *AfeI* enzyme digestion to produce NH_2-terminus-S1−S2−S3, NH_2-terminus-S1−S2−S3−S4−S5, or NH_2-terminus-S1−S2−S3−S4−S5−S6-proximal C-terminus, respectively. Proteins were translated in vitro with [^{35}S]methionine (2 μL/25 μL translation mixture; ∼10 μCi/μL Express, Dupont/NEN Research Products, Boston, MA) for 15−120 min at either 22 or 30 °C in the presence of canine microsomal membranes in rabbit reticulocyte lysate according to the Promega Protocol and Application Guide.

Sucrose Gradients. Twenty-five microliters of translation product (containing membranes) were centrifuged through a sucrose cushion (100 μL; 0.5 M sucrose, 100 mM KCl, 5 mM $MgCl_2$, 50 mM Hepes, 1 mM DTT, pH 7.5) for 5 min at 55 000 rpm at 4 °C. The pellet was resuspended in Hepes buffer (200−300 μL) containing 200 mM NaCl, 2 mM EDTA, 1 mM DTT, 20 mM Hepes, pH 8.0−8.4, and 0.05% dodecylmaltoside (C_{12}M), and kept on ice for 1 h. The solution was centrifuged at 60 000 rpm for 60 min and the supernatant loaded on the top of a 5−20% sucrose Hepes buffer gradient column, spun at 36 000 rpm in a SW40T rotor for 20 h at 4 °C. Fractions (0.35 mL) were collected and precipitated with trichloroacetic acid and analyzed by SDS−PAGE. The fractional migration was calibrated using molecular weight standards: carbonic anhydrase (MW = 29 kD), bovine serum albumin (MW = 66 kD), fumerase (MW

= 206 kD), and catalase (MW = 250 kD). In those experiments designed to detect both ribosomes and *BstEII*-cut nascent peptide, translations (22 °C for 2 h with membranes) were quenched with either puromycin (1 mM) or cyclohexamide (30 μg/mL) and incubated for an additional 15 or 10 min, respectively, at 22 °C, then diluted into buffer containing 50 mM NaCl, 20 mM Hepes, pH 7.3, 0.05% $C_{12}M$, 1 mM $MgCl_2$, 1 mM DTT, 0.1 mM phenylmethanesulfonyl fluoride (PMSF), 10 μg/mL bovine serum albumin, incubated on ice for 30 min, and loaded onto an 11-mL 5−30% sucrose gradient. The gradient was centrifuged for 3 h at 4 °C at 36 000 rpm in a Beckman L-80 ultracentrifuge. Fractions (0.5 mL) were collected, measured for absorbance at 254 nm to detect RNA and also precipitated with trichloroacetic acid and analyzed by LDS−NUPAGE to detect protein.

Gel Electrophoresis and Fluorography. Electrophoresis was performed using the NUPAGE system and precast Bis-Tris 10% or 4−12% gels. Gels were soaked in Amplify (Amersham Corp., Arlington Heights, IL) to enhance ^{35}S fluorography, dried, and exposed to Kodak X-AR film at −70 °C. Typical exposure times were 16−30 h. Quantitation of gels was carried out directly using a Molecular Dynamic PhosphorImager (Sunnyvale, CA), which is very sensitive and detects cpm that are not necessarily visualized in autoradiograms exposed for 16−30 h. Thus, some bands, at the level of 5−10% of the protein, are not visible but are detected by PhosphorImaging.

Oocyte Expression and Electrophysiology. Oocytes were isolated from *Xenopus laevis* females (Xenopus I, Michigan) as described previously (*14*). Stage V−VI oocytes were selected and microinjected with ∼0.1 ng of cRNA encoding for wild-type or mutant Kv1.3. K^+ currents from cRNA-injected oocytes were measured by two-microelectrode voltage clamping using a OC-725C oocyte clamp (Warner Instrument Corp., Hamden, CT.) after 24−48 h, at which time currents were 2−10 μA. Electrodes (<1 MΩ) contained 3 M KCl. The currents were filtered at 1 kHz. The bath Ringer solution contained (in mM): 116 NaCl, 2 KCl, 1.8 $CaCl_2$, 2 $MgCl_2$, 5 Hepes (pH 7.6). The holding potential was −100 mV. For experiments in which inactivation kinetics were determined, we fit the data at +50 mV using the simplex algorithm (Clampfit, Axon Instruments).

For membrane protein assays, oocytes were injected with 60 ng of cRNA encoding pSP/Kv1.3/ C1−$C5^-$/C6−$C9^+$/ C10−$C12^-$/R118C/D126C/Flag along with ^{35}S-methionine (20 μCi).

Cross-Linking. Translation reaction was diluted (1:100) into PBS (pH 7.3, no DTT) and ortho-phenyldimaleimide (*o*-PDM, 0.5 mM; Sigma, St. Louis, MO) added and incubated for 60 min at 4 °C. The mixture was quenched with DTT (5 mM) and centrifuged through a sucrose cushion (120 μL, 0.5 M sucrose, 100 mM KCl, 50 mM Hepes, 5 mM $MgCl_2$, 1 mM DTT, pH 7.5) at 50000*g* for 7 min. The pellet was collected and solubilized in loading buffer and run on LDS−NUPAGE gel (Bis-Tris, 4−12%). For samples generated in the absence of microsomal membranes and in the presence of puromycin or detergent, protein was precipitated with trichloroacetic acid and then solubilized for LDS−NUPAGE analysis. To determine the optimum conditions for these cross-linking experiments, we varied the time of translation, *o*-PDM concentration and incubation time (data not shown) to maximize multimer formation. The conditions used in all the experiments were 3 h for translation at 22 °C, cross-linking with *o*-PDM at 0.5 mM for 60 min at 4 °C. In some cases, the translation mixture was first pelleted through a sucrose cushion, resuspended, and cross-linked with *o*-PDM. When oxidants were used, the same procedure was followed, except that GSSG (2mM), H_2O_2 (0.2%), or air was mixed into the PBS solution and incubated at room temperature (GSSG for 60 min, H_2O_2 and air for 20 min). In these cases, loading buffer did not contain any reducing agent, nor did the running buffer in the LDS−NUPAGE system.

Cross-linking of oocyte membrane preparations was carried out as follows. Oocyte membrane pellets (10∼15 oocytes/reaction) were resuspended in PBS (pH 7.6) and rapid cross-linking was induced by treatment with 0.1% H_2O_2 for 2−5 min at room temperature. The reactions were terminated by addition of 20 mM NEM.

Puromycin Experiments. To release the Kv1.3 peptide from tRNA, we added puromycin (Sigma Chemical Co., St. Louis, MO) to the translation reaction at a final concentration of 1 mM and incubated the mixture for 15−60 min at 22 °C. These experiments were conducted in both the absence and presence of microsomal membranes in the translation mixture and the subsequent analyses used LDS−NUPAGE gels, run under both alkaline and neutral conditions.

Oocyte Membrane Preparation and Coimmunoprecipitation. Oocytes (10−15 per lane) were homogenized under reducing conditions in 100−200 μL of HEDP buffer (100 mM Hepes-NaOH, pH 7.6, 1 mM EDTA, 5 mM DTT, PMSF 100 μg/mL) and kept at 4 °C during all subsequent steps. Following centrifugation (3000*g*, 10−15 min), the supernatant was collected and the pellet was vigorously resuspended in 100−200 μL HEDP. Centrifugation was repeated and the supernatant (200−400 μL) combined with the previous supernatant. The homogenate was overlaid on a 15% sucrose cushion prepared in 100 mM Hepes-NaOH (pH 7.6) followed by centrifugation (55000*g*, 75 min at 4 °C). The membrane pellet was resuspended in PBS (pH 7.6). For immunoprecipitation, membrane pellets were diluted into 1 mL of buffer A (0.1 M NaCl, 0.1 M Tris (pH 8.0), 10 mM EDTA, 1% Triton X-100, and 1 mM PMSF) and incubated on ice for 1−2 h. Following centrifugation (55000*g*, 60 min), the supernatant was collected and mixed with 15 μL mouse IgG-agarose beads (Sigma Chemical Co., St. Louis, MO) and incubated at 4 °C for 60 min. After centrifugation (14000g, 2−5 min), the supernatant was collected and incubated with mouse anti-Flag-M2-agarose beads (10∼15 μL; Sigma Chemical Co., St. Louis, MO) at 4 °C on a rotator overnight. The samples were centrifuged, the pelleted beads washed 3× with buffer A and twice with 0.1 M NaCl, 0.1 M Tris, (pH 8.0), and then analyzed by LDS−NUPAGE gel.

RESULTS

Cross-Linking Full-Length Kv1.3. We created Kv1.3 clones lacking cytosolic N- and C-terminal native cysteines (see Materials and Methods) and introduced cysteine pairs into the intersubunit T1−T1 interface. Using these constructs, we tested whether these pairs could be cross-linked in tetrameric Kv1.3 that was translated in vitro and integrated into microsomal (ER, endoplasmic reticulum) membranes.

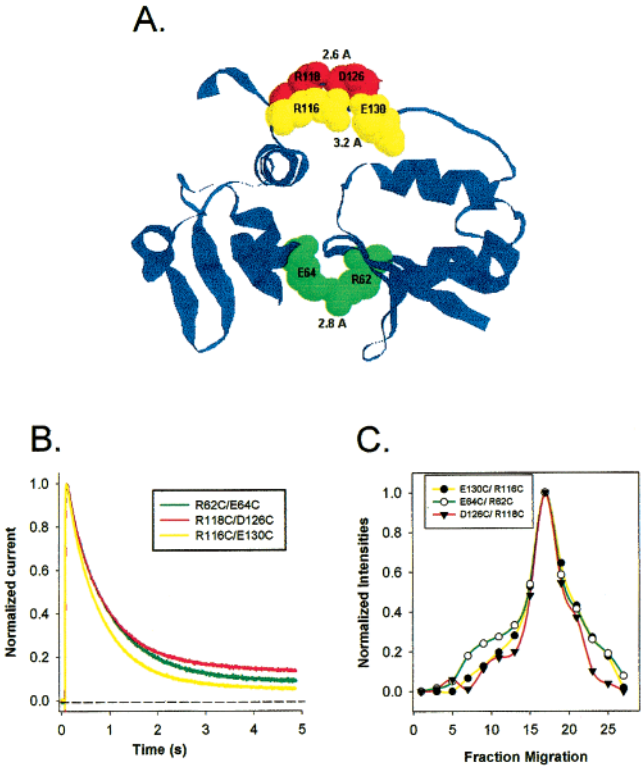

FIGURE 1: Engineered cysteines in mutated, full-length Kv1.3 in ER membranes. (A) Ribbon representation of two adjacent subunits of Kv1.1a, taken from the crystal structure (*11*). Pairs of residues at the T1−T1 interface, R132/D140, R130/E144, and R76/E78 in Kv1.1a, are depicted as spacefilling molecules and labeled as the equivalent Kv1.3 residues R118/D126 (red), R116/E130 (yellow), and R62/E64 (green), respectively. Distances between indicated residues are given in angstoms. The last 10 amino acids on each subunit are omitted for clarity. (B) Function and assembly assays. *Xenopus* oocytes were injected with cRNA for full-length R118C/D126C, R116C/E130C, and R62C/E64C and recordings were made 24−48 h postinjection. Peak current at +50 mV was measured to give the current trace shown on the left. The inactivation time constants (750, 700, and 840 ms, respectively) are similar to those of wild-type Kv1.3 (*55*). (C) Fractional migration of engineered Kv1.3 constructs in a sucrose gradient. Full-length R118C/D126C, R116C/E130C, and R62C/E64C were each translated in vitro (Materials and Methods) and solubilized in 0.05% $C_{12}M$, sedimented through a 5−20% sucrose gradient at 4 °C for 20 h at 36 K rpm. Only odd-numbered fractions (0.35 mL) are shown in the figure and fractional migration is plotted as cpm normalized to the maximum cpm for each construct. The fractional migration was calibrated using molecular weight standards: carbonic anhydrase (MW = 29 kD), bovine serum albumin (MW = 66 kD), fumerase (MW = 206 kD), and catalase (MW = 250 kD). Predicted fractional migration for Kv1.3 monomer are fractions 5−7 and for the tetramer, fractions 17−19.

Kv1.3 forms tetramers in ER membranes (*15*, *16*). The engineered pairs we selected were R118C/D126C, R116C/E130C, and R62C/E64C (Figure 1A). The equivalent residues of these pairs in *Shaker* were also chosen by Miller and co-workers (*9*) to show the existence of a *Shaker* T1-structure in the plasma membrane of *Xenopus* oocytes. The intersubunit distance between native side-chains in each pair is within 2.5−3.2 Å, as derived from crystallographic determinations of Kv1.1a, *Shaker* and Kv1.2 (*11*−*13*). Each of the Kv1.3 constructs containing engineered pairs gave functional channels when expressed in *Xenopus* oocytes (Figure 1B) and tetramers in sucrose density gradient measurements (Figure 1C).

Although the intersubunit distance between the side chains of substituted cysteines need not have the same proximity as the native residues, we assumed that a bifunctional cross-linker might still be capable of cross-linking each pair of engineered cysteines. The engineered full-length R118C/D126C was translated in vitro to give protein that appears as a broad band containing a doublet on LDS−NUPAGE gels (unglycosylated and core glycosylated (*17*)) at the predicted molecular weight of the monomer, 58 kD. The translation reaction was then treated with the bifunctional cross-linker ortho-phenyldimaleimide (*o*-PDM, Sigma, St. Louis, MO) (*18*). The distance between the functional maleimide groups is ∼6 Å. As shown in Figure 2A, significant cross-linking was obtained such that the fraction of protein detected as dimers and trimers/tetramers was 22 and 47%, respectively. These results suggest that the side chains within each pair approach each other within 6 Å and that the T1 structure may already exist in full-length Kv1.3 in the ER membrane. Could these residues be even closer than 6 Å? We therefore treated these pairs with hydrogen peroxide (H_2O_2, 0.2%) or oxidized glutathione (GSSG, 2 mM) and then treated the final samples with either reducing (50 mM DTT) or nonreducing (no addition) loading buffer and analyzed them by LDS−NUPAGE. GSSG was included because it is the principal redox buffer in the ER under normal physiological conditions and obviates free radical-induced misfolding and aggregation (*19*). GSSG supports proper posttranslational folding over a wide range of concentrations (2−20 mM) without "overoxidation", which is a common problem of other artificial oxidizing agents (e.g., iodine, diamide). Both reagents cross-linked ∼30−40% of total full-length R118C/D126C to give dimers and multimers (Figure 2A). The fraction of protein detected as dimers and combined trimers/tetramers is, respectively, 20 and 21% using H_2O_2 oxidation, and 21 and 15% using GSSG. These results suggest that the side chains of residues R118C and D126C can approach one another within 2 Å. For both *o*-PDM and oxidizing experiments, control constructs containing only one cysteine of the engineered pair did not cross-link to produce oligomers (data not shown, but see Figure 5 below).

To test whether these in vitro observations reflect N-terminal proximity in the ER in vivo, we performed a similar experiment using *Xenopus* oocytes injected with full-length R118C/D126C and harvested at the times indicated in Figure 2B. The left panel (lanes 1−4) shows a time course of expression. The sharp band at 58 kD is full-length core glycosylated Kv1.3, which was made in the ER and can be detected as early as 3 h (also see refs *20*). Longer times produced a higher molecular weight species (∼70 kD), which represents further processing by other compartments after Kv1.3 exits the ER (*20*). Brefeldin A (BFA, Sigma Chemical Co., St. Louis, MO; 5 μg/mL) blocks exit of Kv1.3 from the ER (lane 5). The right panel shows the results of H_2O_2 oxidation (0.1%). Virtually all of the protein is cross-linked to give tetramers (∼232 kD; lanes 6, 8, and 9), which can be reduced with DTT (50 mM, lanes 7 and 10). Trace bands are detectable at the dimer and trimer molecular weights (∼116 and 174kD, respectively; lanes 8 and 9). Even the 3-h postinjection measurement indicates DTT-reducible tetramers are present. Neither full-length R118C nor full-

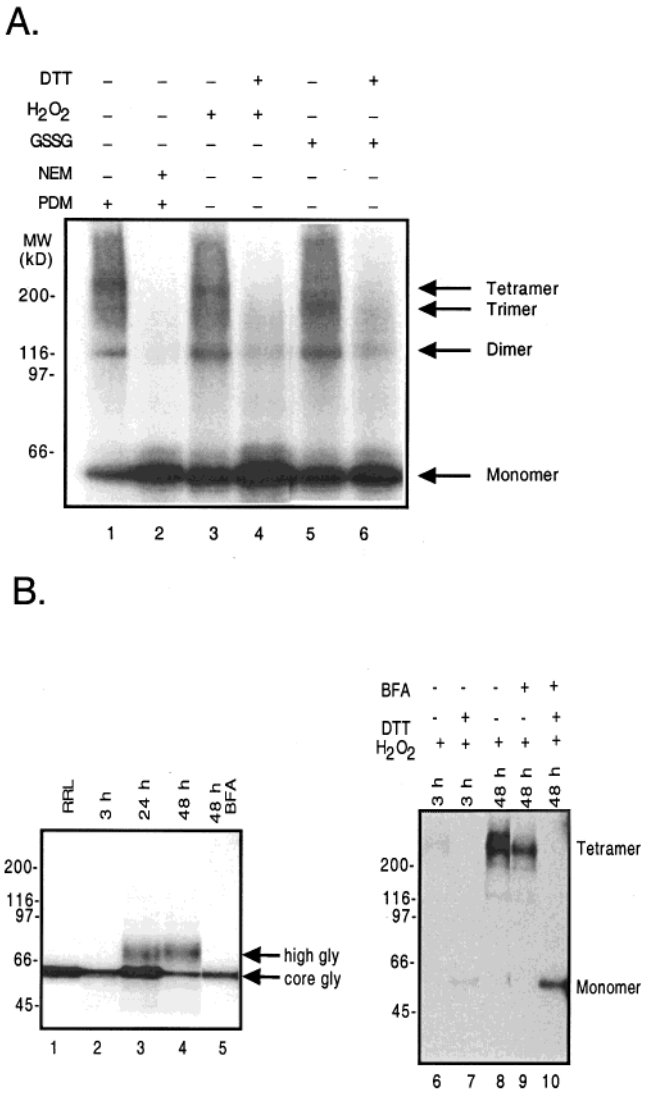

FIGURE 2: Cross-linking of engineered cysteines in mutated, full-length Kv1.3 in ER membranes. (A) In vitro, full-length R118C/D126C was translated and incubated with either 0.5 mM *o*-PDM (lanes 1 and 2), 0.2% H_2O_2 (lanes 3 and 4), or 2 mM GSSG (lanes 5 and 6). Samples cross-linked with *o*-PDM were pretreated with nothing (lanes 1) or with NEM (20 mM; lanes 2). Samples subjected to oxidants were solubilized in loading buffer containing either no DTT (lanes 3 and 5) or 50 mM DTT (lanes 4 and 6). (B) Full-length R118C/D126C expressed in *Xenopus* oocytes and cross-linked under oxidizing conditions. Left: Time course of full-length R118C/D126C expressed in *Xenopus* oocytes. RRL indicates in vitro translation of full-length R118C/D126C in rabbit reticulocyte lysate and microsomal membranes. Only core glycosylation occurs in this case. BFA indicates that oocytes were incubated with Brefeldin A (5 μg/mL; lanes 5), which prevents protein exit from the ER. Consequently, protein only exhibits core glycosylation and not higher glycosylation. Right: Membranes were isolated and exposed to 0.1% H_2O_2 as described in the Materials and Methods. Some oocytes were incubated continuously with BFA (5 μg/mL) to trap newly formed Kv1.3 in the ER (lane 9). Loading buffer contained either no DTT or 50 mM DTT, as indicated above each lane.

length D126C injected alone produced any cross-linked products (data not shown). In BFA-treated oocytes, the expressed full-length R118C/D126C is clearly an ER-resident protein. Thus, in vivo in the ER, residues R118C and D126C in neighboring subunits already approach each other within 2 Å, thereby supporting the validity of the in vitro microsomal membrane preparation.

Kv1.3 Translocation Intermediates. We have hypothesized that NH_2-termini of nascent subunits associate early in biogenesis, perhaps while the nascent subunits are still attached to ribosomes. To test this hypothesis, we used the engineered pair R118C/D126C to construct a translation intermediate, i.e., a truncated Kv1.3 fragment that lacks a stop codon and remains attached to ribosomes. The fragment was made using the restriction enzyme *BstEII* to create linearized R118C/D126C/Kv1.3 DNA templates for making the in vitro transcribed cRNA. The resulting Kv1.3 segments retained in the construct are depicted in Figure 3A. *BstEII*-cut R118C/D126C/Kv1.3 was translated and solubilized in either pH 8.6 (Figure 3B, lanes 1 and 2) or pH 7.0 (lanes 3 and 4) loading buffer and run on LDS−NUPAGE (respectively, with running buffers of pH 7.7 or 7.3) at 4 °C for 2 h (125 V). At both pHs, the monomeric peptide band appears as a doublet at the predicted molecular weight of 43 kD. The upper band is due to ER core glycosylation; the lower one is unglycosylated Kv1.3 (*21*). Thus, this protein translocates across the membrane. An additional band appears at ~60 kD, which, with good gel resolution, also presents as a doublet of glycosylated and unglycosylated species. The ~17-kD higher bands are consistent with them being peptidyl-tRNA complexes, which are pH-sensitive and dissociate more readily at alkaline pH. This assignment is confirmed by the collapse of these higher molecular weight bands into a single 43-kD band after incubation (60 min, 22 °C) with puromycin (1 mM), which releases the peptide from the tRNA (*22*, *23*). This band is absent in control translations in which mRNA is absent (lane 5), and this band disappears, concomitant with an increase in the peptide band, when the sample is treated with RNase (lane 7). For comparison with the *BstEII*-cut Kv1.3, a full-length control R118C/D126C/Kv1.3 construct that contains a stop codon does not have such a peptidyl-tRNA band (Figure 2A, lanes 1 and 2).

Finally, almost all of the nascent peptide is attached to the ribosome as shown by the following two experiments. Translation of *BstEII*-cut R118C/D126C/Kv1.3 in the absence of microsomal membranes gives a product that pellets with high-speed centrifugation (70000*g*) of the translation reaction (Figure 3C, lanes 1 and 2). Under these conditions, only polysomes will pellet. Free peptide or free peptidyl-tRNA will remain in the supernatant. The pelleted fraction contains 95% of the R118C/D126C/Kv1.3 protein. In contrast, the translation product generated in the absence of membranes but in the presence of puromycin is mostly (60%) in the supernatant (lanes 3 and 4). To confirm that *BstEII*-cut R118C/D126C/Kv1.3 nascent peptide is still attached to ribosomes in the presence of membranes, we subjected the translation product to sucrose gradient centrifugation, monitoring the fractions for absorbance at 254 nm to detect RNA and for migration on LDS−NUPAGE to detect nascent peptide (Figure 3D). All of the peptide comigrates with RNA (both peaks occur at fractions 13−14) and displays a strong peptidyl-tRNA band at ~60 kD.[1] In contrast, puromycin-released peptide migrates in fractions 2−4 (displaying no peptidyl-tRNA band) while RNA still appears only at fractions >11. Moreover, the peptide that comigrates with

[1] This suggests that the monomer band was generated from peptidyl-tRNA by electrophoresis. If free monomer were present in the reaction mixture, it would have migrated at the top of the gradient.

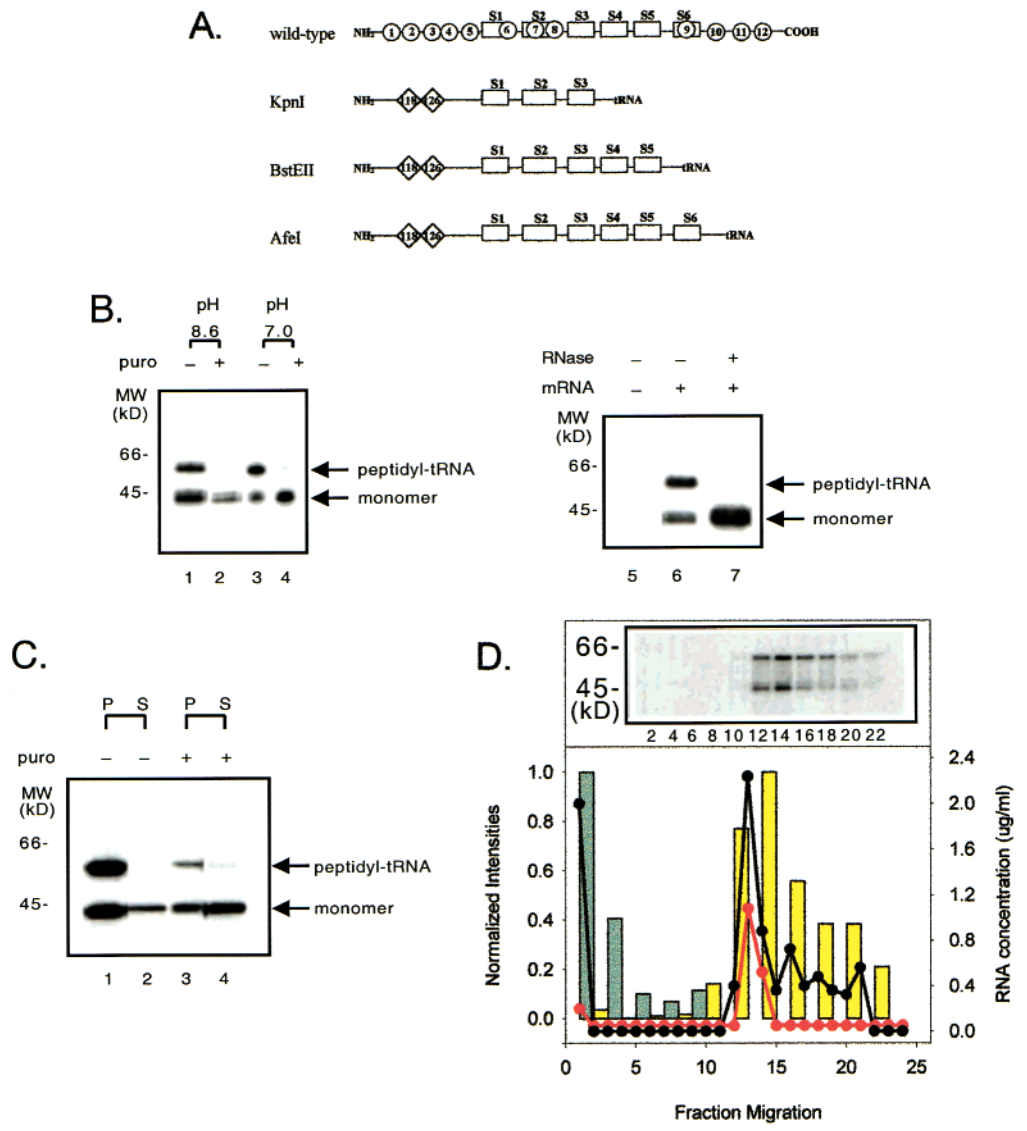

FIGURE 3: Validation of the translocation intermediates. (A) Schematic of translocation intermediates generated by restriction enzymes *KpnI*, *BstEII*, and *AfeI*. For reference, wild-type Kv1.3 is shown with its 12 native cysteines, labeled C1−C12 in circles. R118C/D126C, containing only two engineered cysteines (diamonds) is shown for *KpnI*-, *BstEII*-, and *AfeI*-cut intermediates. The last amino acid in each construct is G292, V387, and S488, respectively. The boxes represent the transmembrane segments, S1−S6. (B) Release of nascent peptide from tRNA. R118C/D126C was translated as described in Materials and Methods, then incubated either in the absence (lanes 1 and 3) or presence of 1 mM puromycin (lanes 2, 4), and then solubilized in either pH 8.6 or pH 7.0 (lanes 1, 2, and 3, 4, respectively) loading buffer, and run on LDS−NUPAGE. The right panel shows the results from a control translation reaction in which mRNA is absent (lane 5) and one containing R118C/D126C mRNA (lane 6) that was treated with 5 μg/mL RNase for 15 min at 37 °C (lane 7). The gels are 4−12% gradient BisTris gels. (C) Ribosome-attached nascent peptide. *BstEII*-cut R118C/D126C was translated in the absence of membranes, incubated in the absence (lanes 1 and 2) or presence (lanes 3 and 4) of 1 mM puromycin and centrifuged at 55000*g*. Pellet protein (P, lanes 1 and 3) was solubilized directly in loading buffer; supernatant protein (S, lanes 2 and 4) was first precipitated with trichloroacetic acid and then dissolved in loading buffer. (D) Sucrose gradient sedimentation of *BstEII*-cut R118C/D126C. Translations of *BstEII*-cut R118C/D126C were quenched with either puromycin (1 mM) or cyclohexamide (30 μg/mL), solubilized in $C_{12}M$, and run on a 5−30% sucrose gradient, as described in Materials and Methods. The RNA concentration (right ordinate, curves) and fraction of total protein (left ordinate, bar histogram) are plotted as a function of fractional migration in the gradient (abscissa) for puromycin (gray bars for peptide) and cyclohexamide (filled black circles for RNA, yellow bars for peptide). The 80S ribosome peak occurs at fraction 13. This was verified by RNase-treatment (filled red circles) and puromycin-treatment (not shown), each provides a marker for a single, 80S ribosome. The faster migrating RNA peaks (fractions 16−22) represent polysomes. Inset: LDS−NUPAGE gel (10%, MOPS buffer) of sucrose gradient fractions for cyclohexamide-quenched translation. Nascent peptide appears as a doublet at 43 kD and peptidyl-tRNA appears as a doublet at ~60 kD.

ribosomes is glycosylated (note doublet of bands at 43 kD, inset), indicating that this peptide was in contact with both the ribosome and the ER membrane. It is also noteworthy that polysomes (2−4 ribosomes per RNA) are present (fractions 16−22), as well as single-ribosome mRNA strands (fraction 13, 80S ribosome peak).[2] Taken together, the results of Figure 3 suggest that translation of *BstEII*-cut R118C/D126C/Kv1.3 generates a nascent peptide that is not only a translation intermediate, but also a translocation intermediate (*24*), and that 95−100% of it is still attached to the ribosome-tRNA complex in the absence or presence of membranes, respectively.

[2] Puromycin-treatment provides a marker for 80S ribosomes. RNase cleaves the mRNA holding multiple ribosomes together, thereby producing only single ribosomes.

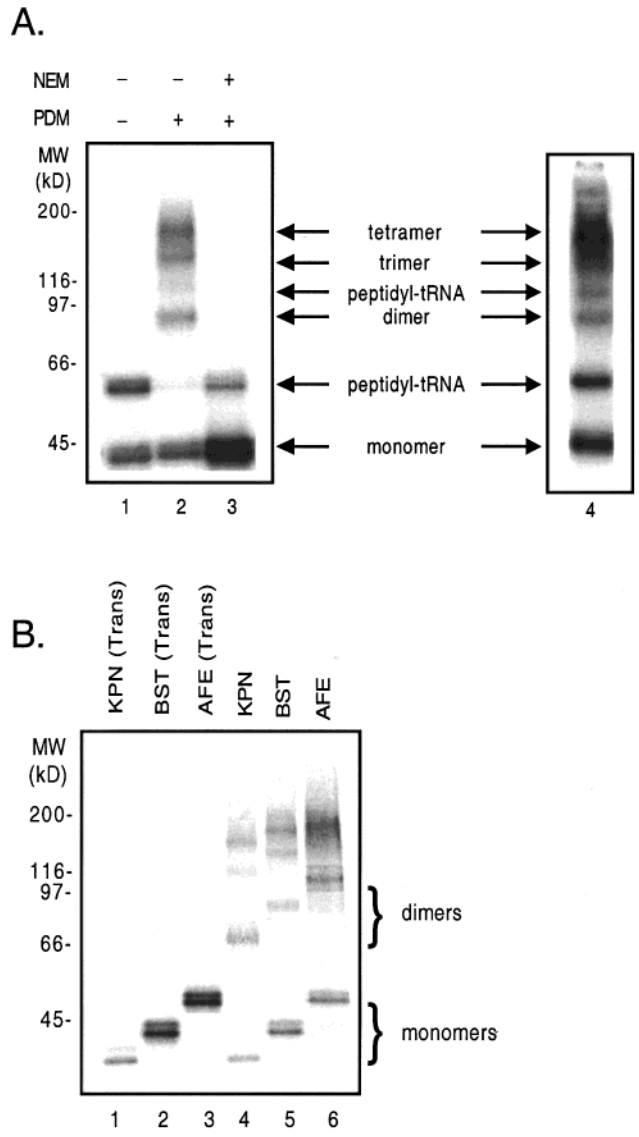

FIGURE 4: Cross-linking of engineered translocation intermediates in ER membranes. (A) *BstEII*-cut R118C/D126C was translated (lane 1) and cross-linked with 0.5 mM *o*-PDM (lanes 2). Pretreatment with NEM (20 mM, 2 h, 4 °C) blocked formation of multimeric species (lane 3). Lane 4 shows cross-linking of membrane-associated intermediates solubilized in $C_{12}M$ (same buffer used in the experiment shown in Figure 3D). (B) *KpnI*-cut (lanes 1, 4), *BstEII*-cut (lanes 2 and 5), and *AfeI*-cut R118C/D126C (lanes 3 and 6) were translated and cross-linked with *o*-PDM. For each construct, the band corresponding to the dimer occurs at the predicted dimer molecular mass, i.e., 64, 90, and 116 kD for *KpnI*-cut, *BstEII*-cut, and *AfeI*-cut R118C/D126C, respectively. RNase (5 μg/mL) was added to the samples after cross-linking to remove peptidyl-tRNA bands.

Cross-Linking Ribosome-Attached Intermediates. We could now address the question of whether amino-terminal interactions occur between independent nascent peptides on different ribosomes. We used the same strategy as for the full-length Kv1.3 tetramers, namely, a bifunctional cross-linker to trap interacting amino-termini of neighboring Kv1.3 translocation intermediates (Figure 4A). *BstEII*-cut R118C/D126C/Kv1.3 was translated in the presence of membranes (lane 1), incubated with *o*-PDM (lane 2), quenched, and run on LDS−NUPAGE gels to give the results shown in Figure 4A. The monomer appears as a band at an apparent molecular weight of 43 kD (monomer). Lane 2 shows additional bands, one at 90 kD, approximately twice the molecular weight of *BstEII*-cut monomer, as well as bands at the molecular weights corresponding to trimer (130 kD) and tetramer (172 kD). Pretreatment with NEM prevents multimer formation (lane 3). Similar results were obtained (cf. lanes 2 and 4) when cross-linking was performed in the same buffer used to demonstrate that the nascent translocation intermediate remains attached to both ribosome and membrane (Figure 3D). Thus, cross-linked products are derived from peptide originally attached to a tRNA/ribosome/membrane complex.

To establish that these higher molecular weight bands reflect pure Kv1.3 multimers and not a cross-linked product of a Kv1.3 monomer with another unrelated protein present in the reaction mixture, we used a mass-tagging strategy as follows. In addition to *BstEII*-cut Kv1.3, we created Kv1.3 translocation intermediates of shorter and longer C-terminal lengths using *KpnI* and *AfeI* restriction enzymes to create linearized R118C/D126C/Kv1.3 DNA templates for making the in vitro transcribed cRNA. The Kv1.3 segments retained in the resulting constructs are depicted in Figure 3A. The predicted molecular weights of the shorter and longer peptides are 32 and 54 kD, respectively. Bands corresponding to these molecular weights were observed upon translation of the cRNA derived from the *KpnI*-cut and *AfeI*-cut cDNA templates (Figure 4B, lanes 1 and 3, respectively). For clarity, these samples were treated with RNase before loading on the gel in order to eliminate the peptidyl-tRNA bands and facilitate a more accurate assessment of the shifted molecular weight of the dimers. Also, note that each monomer appears as a doublet of unglycosylated and core glycosylated peptide. Treatment of *KpnI*-, *BstEII*-, and *AfeI*-cut Kv1.3 with *o*-PDM produced cross-linked products at ~68, 88, and 110 kD, as well as at higher molecular weights (116, 130, 160, corresponding to trimer for *KpnI*-, *BstEII*-, and *AfeI*-cut; 130, 180, 200, corresponding to tetramer, respectively, for each construct; lanes 4−6). For each construct, the dimer band is always located at a molecular weight that is twice that of the monomer, thereby confirming that the cross-linked dimer is not a product of Kv1.3 and another, unrelated protein. The latter scenario would result in a constant gel shift regardless of the molecular weight of the Kv1.3 monomer. Two different protocols were used in these experiments. In one, we centrifuged the translation reaction mixture to pellet the ribosome-attached membranes containing the nascent Kv1.3, resuspended the membranes and added *o*-PDM. In the other method, we took an aliquot of the translation reaction mixture and diluted it, 20×, 50×, or 100×, into a phosphate-buffered saline buffer and added *o*-PDM. In all cases, the same cross-linked multimers were detected in the same relative ratios (data not shown), consistent with the cross-linked peptides originating on the same membrane vesicle and/or polysome, and engaged in true Kv1.3 self-association. These results confirm that we are cross-linking Kv1.3 monomers, most likely attached to polysomes. Moreover, these results suggest that the proximity of the N-termini and the ability to cross-link them are independent of chain length in the range of 32 to 54 kD of the protein. The minimum length has not yet been determined; however, a minimum of 60−80 amino acids is necessary for the nascent peptide to emerge from the ribosome (*25*).

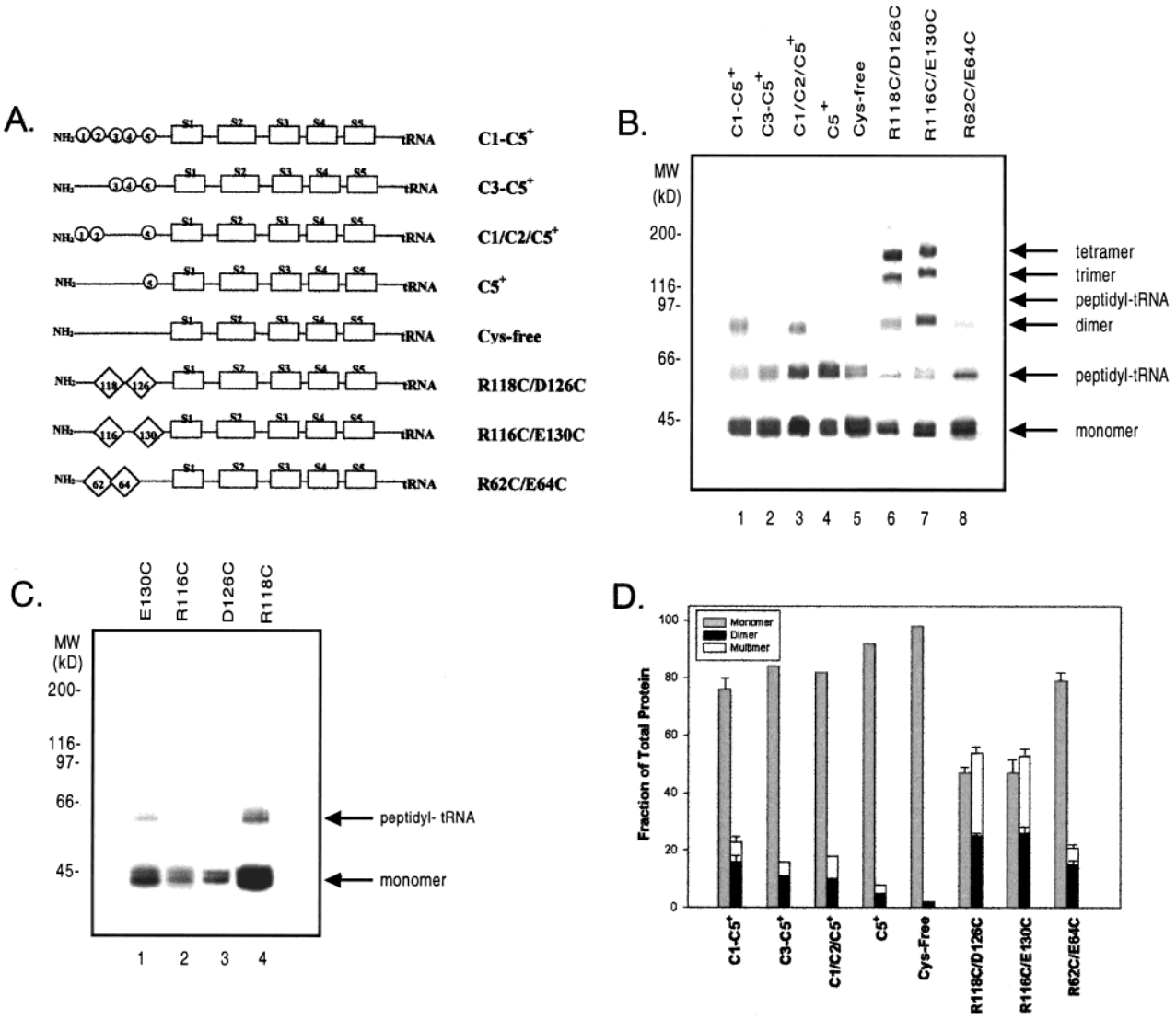

FIGURE 5: Residue specificity of PDM-cross-linking. (A) Schematic diagram of *BstEII*-cut translocation intermediate constructs. Native cysteines are shown as circles; C1−C5 indicate the native cysteines in Kv1.3, other numbers (in diamonds) indicate the position of the native residue that has been mutated to a cysteine. The absence of native cysteines C1−C8 indicates that they have been mutated to alanine, valine, or serine, as stated in Materials and Methods. The last amino acid in the *BstEII*-cut constructs is V387. (B) *o*-PDM-mediated cross-linking of *BstEII*-cut constructs. Each construct was translated in the presence of microsomal membranes and cross-linked with 0.5 mM *o*-PDM as described in Materials and Methods. (C) *o*-PDM-mediated cross-linking of *BstEII*-cut constructs containing a single cysteine. R118C (lane 4), D126C (lanes 3), R116C (lane 2), E130C (lane 1) were translated and cross-linked with 0.5 mM *o*-PDM. (D) The percent of total *BstEII*-cut Kv1.3 that is monomer (gray bar), dimer (black bar), or trimer plus tetramer (white bar). Data are mean ± SEM for those data represented with error bars. For C1−C5$^+$, R118C/D126C, R116C/E130C, and R62C/E64C, the number of experiments was $n = 3$, 25, 6, and 7, respectively. For the other constructs, the data represent one experiment or the average of two experiments.

Specificity of T1−T1 Interactions. Having shown that the N-termini of Kv1.3 nascent peptides can be cross-linked in the ER while attached to ribosomes, we asked whether the proximity of the N-termini is due to specific T1−T1 interactions. For a number of constructs containing different numbers of cysteines in different positions in the Kv1.3 N-terminus (Figure 5A), we conducted identical cross-linking experiments. All of the constructs were made in a cysteine-free background and contain only the indicated cysteines. Some of these constructs contain native Kv1.3 cysteines (numbers in circles), others were engineered (numbers in diamonds), including the three paired-cysteine mutations shown in Figure 1A. These constructs were cross-linked, as were several control peptides containing only one of the paired residues. The engineered pairs, R118C/D126C, R116C/E130C, and R62C/E64C, contain no native cysteines and only the respective two cysteines (indicated by diamonds).

As shown in Figure 5B, *o*-PDM-treatment produced strong bands at the dimer, trimer, and tetramer positions for R118C/D126C and R116C/E130C (lanes 6 and 7). This was true even for the similar construct, R118C/D126C/core cysteines C6−C9$^+$, which contains the engineered pair of cysteines plus native C6, C7, C8, and C9 in the transmembrane segments S1−S6 (data not shown). All other constructs exhibit <18% of the protein as dimer bands and only trace amounts of higher molecular weight multimers. Peptides containing only the single mutation of an engineered pair did not produce significant cross-linking (Figure 5C). These results were quantitated using PhosphorImager analysis (Figure 5D) and indicate that cross-linking either R118C/D126C pair or R116C/E130C pair produces ≥25% of the protein as dimers and ≥30% as a mixture of trimers and

tetramers, whereas even those peptides containing three cysteines (constructs C3−C5$^+$ and C1/C2/C5$^+$) or five cysteines (construct C1−C5$^+$) produce ≤15% of the protein as dimers and ≤7% as a mixture of trimers and tetramers. The Cys-free peptide produces only monomer. Although cross-linking appears to be specific for interfacial T1 residues, the corollory is not true, i.e., not all pairwise residues at the T1 interface can be cross-linked, similar to the observations reported by Miller and co-workers (*9*). For example, R62C/E64C produces only 15% of the protein as dimers and 7% as a mixture of trimers and tetramers. To summarize, the cross-linking observed for R118C/D126C and R116C/E130C is specific, and these paired residues can approach within 6 Å of each other while still attached to the ribosome. This suggests that cross-linked residues are located at the interface of a folded T1 domain, rather than arising by cross-linking of random cysteines in an unfolded NH_2-terminus.

Intrinsic T1−T1 Interactions. The propinquity of these T1 residues could be due to intrinsic interactions between the side chains or to ribosomes and/or membranes holding the side chains in close proximity. To distinguish these possibilities, we added puromycin to the completed *BstEII*-cut translation reactions and cross-linked the products as previously described. As shown in Figure 6A, regardless of whether the peptidyl-tRNA complex is cross-linked first (lane 3) or the peptide is released first (lanes 2 and 4) and then cross-linked, the oligomeric products are the same (lanes 3 and 4). Note that the peptidyl-tRNA band (∼60kD) is absent when cross-linking is preceded by puromycin treatment, yet the cross-linked bands remain (cf. lanes 3 and 4). These results suggest that the ribosomes do not hold the N-termini together, but rather that the N-terminal interaction persists even after the peptide is released from the ribosome.

Is it possible that the membrane holds the N-termini of nascent peptides together? To address this issue, we investigated the role of the membrane in permitting N-termini of nascent chains to come within efficient cross-linking distance of each other. Translations and cross-linking experiments were carried out in the presence and absence of microsomal membranes (Figure 6B). The extent of cross-linking is considerably greater in the presence of membranes (lanes 1−4 versus lanes 5−8) for both the bifunctional cross-linker and an oxidant, GSSG (see below, Figure 7)). This suggests that membrane attachment facilitates inter-ribosomal nascent peptide interactions.

A final experiment confirmed that neither ribosomes nor membranes hold N-termini in close proximity. Peptide-containing vesicles were isolated, suspended in a high salt (0.5 M)/high EDTA (25 mM) buffer containing C_{12}M, and then cross-linked. The high salt/EDTA buffer detaches ribosomes, while C_{12}M solubilizes membranes. Cross-linked products were detected in the supernatant only, indicating that free peptides, formerly in a ribosome/tRNA/membrane complex, remained associated in solution through T1−T1 interactions (data not shown; see also Figure 4A, lane 4).

Disulfide-Bond Formation between Engineered Cysteines. Could these specific T1 residues come as close as 2−3 Å as is implied by the crystallographic data for mature tetrameric T1 structures, while still attached to ribosomes? Or does such close proximity require the complete tetrameric channel structure found at a later biogenic stage in the Kv channel of the plasma membrane (*9*)? To explore this possibility, we subjected the *BstEII*-cut translocation intermediate to oxidation conditions and analyzed the results using nonreducing LDS−NUPAGE. The three oxidizing agents were GSSG, H_2O_2, and air (no DTT present). Each of these agents was tested with respect to time and concentration to obtain optimum, nonaggregating conditions (data not shown). The results are presented in Figure 7; an *o*-PDM control, done simultaneously is shown in Figure 4A. Each of the oxidizing agents produced bands corresponding to cross-linked multimers (lanes 1, 3, 5), and each was reduced with DTT to the monomer (lanes 2, 4, 6), albeit GSSG was the most effective under the specified conditions. These results suggest that amino acid side chains in the nascent Kv1.3 peptides, specifically some residues in the T1−T1 intersubunit interface, can approach one another within 2−3 Å at early stages of biogenesis in the ER.

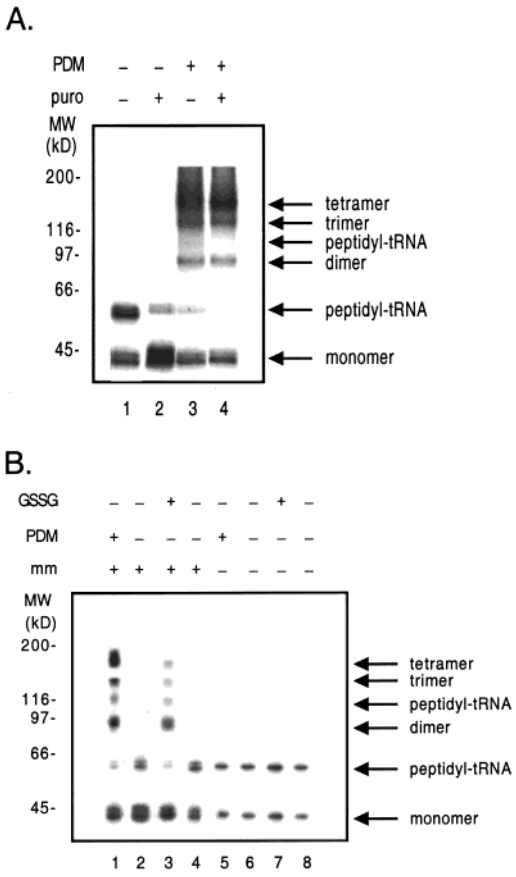

FIGURE 6: Dependence of *o*-PDM-cross-linking on the presence of ribosomes and membranes. (A) *BstEII*-cut R118C/D126C was translated, incubated in the absence (lanes 1 and 3) or presence (lanes 2 and 4) of puromycin (1 mM), and then cross-linked with *o*-PDM (lanes 2 and 4). No RNase was added to the samples, so the peptidyl-tRNA band is still visible in the samples without puromycin (lanes 1 and 2). (B) *BstEII*-cut R118C/D126C was translated in the absence or presence of membranes (mm), cross-linked in the absence or presence of *o*-PDM (0.5 mM), or in the absence or presence of GSSG (2 mM) as described for Figures 2 and 4 and in the Materials and Methods.

Intra- versus Interpolysomal Association. To investigate whether these initial T1-T1 interactions are intra- or interpolysomal, we again used the mass-tagging strategy. *KpnI* and *AfeI* translocation intermediates of R118C/D126C were

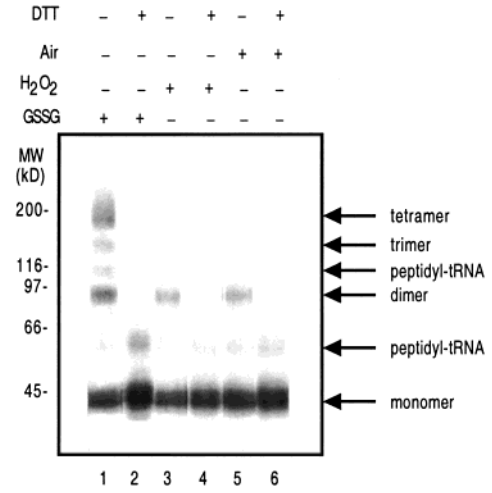

FIGURE 7: *BstEII*-cut R118C/D126C cross-linked under oxidizing conditions. *BstEII*-cut R118C/D126C was translated and incubated with 2 mM GSSG, 0.2% H_2O_2, or air (absence of DTT), as described in Materials and Methods, and then centrifuged through a sucrose cushion and the pellet solubilized in loading buffer containing either no DTT or 50 mM DTT.

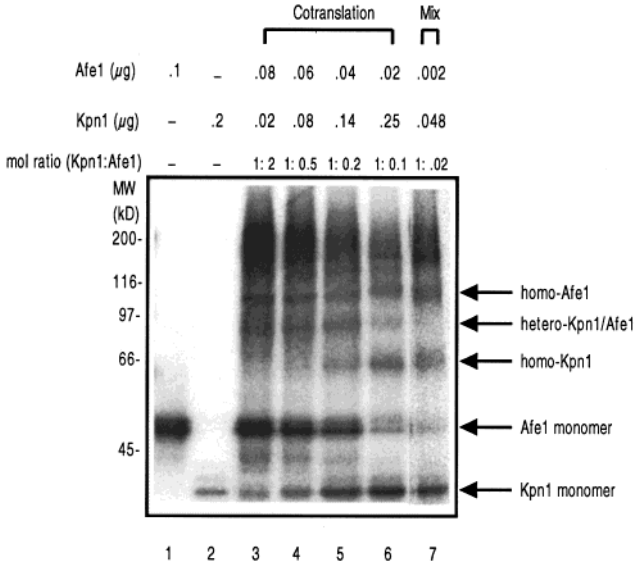

FIGURE 8: Interpolysomal cross-linking. R118C/D126C, *KpnI*-cut and *AfeI*-cut, were co-translated in different molar ratios of mRNA and cross-linked with *o*-PDM (lanes 3−6). The ratio of *AfeI* to *KpnI* was decreased in the co-translations displayed in lanes 3−6. Each construct was also separately translated (lanes 1 and 2), mixed together, and then cross-linked (lane 7). For clarity, RNase was added after cross-linking to eliminate complicating peptidyl-tRNA bands. Dimers are labeled "homo-*KpnI*" (64 kD), "homo-*AfeI*" (108 kD), or "hetero-*KpnI*/*AfeI*" (86 kD). Monomers appear as bands at 32 and 54 kD for *KpnI* and *AfeI*, respectively. The numbers at the top of each lane are the calculated amounts of mRNA added to the translation reaction; the mol ratios were derived from μg of mRNA added, divided by the molecular weight of the construct. N.B. The number of methionines in *AfeI* and *KpnI* differs. The *AfeI* construct contains nine methionines, whereas the *KpnI* construct contains four methionines. Therefore, to compare *KpnI* and *AfeI* intensities, the intensities of *AfeI* monomers and homodimers must be multiplied by 0.44; hetero-*KpnI*/*AfeI* dimers must be multiplied by 0.72 to compare them to *KpnI* homodimers.

translated separately (Figure 8, lanes 1 and 2) or together in different molar ratios to give nascent peptides of 32 and 54 kD, respectively. The co-translated reactions were cross-linked with *o*-PDM (lanes 3−6) and the separately translated reactions were first mixed together and then cross-linked (lane 7). Cross-linking of the co-translation mixture gave homodimers at ∼66 kD (homo-*KpnI*) and 108 kD (homo-*AfeI*), but additionally a relatively strong band at ∼86 kD, consistent with heterodimer formation (hetero-*KpnI*/*AfeI*). This band is not present in the cross-linked mixture of independently translated *KpnI* and *AfeI* peptides (lane 7). Our results show that heterodimers are formed. Heterodimers can only come from cross-linking nascent peptides that were made on two different polysomes. Hence, cross-linking occurs interpolysomally, but this does not preclude intrapolysomal interactions.

Co-translational T1−T1 Association. Finally, to investigate whether T1−T1 proximity is initiated during chain elongation of the nascent protein, we translated BstEII-cut R118C/D126C and cross-linked it with *o*-PDM at the translation times indicated in Figure 9. At the earliest time that protein could be detected (15 min) monomer and monomeric peptidyl-tRNA were present along with a ladder of smaller molecular weight bands, presumably due to shorter, incompletely elongated chains (lane 1). This ladder was diminished but still present at 30−60 min and absent by 120 min (lanes 2−3 and 4, respectively), suggesting that protein continued to be elongated on the ribosome during this time. Visual detection of cross-linking on the gel was clear at 30 min and longer, when large amounts of protein were synthesized (e.g., lanes 6 and 7). All the time points were quantitated using PhosphorImager analysis (Figure 9B). The results show that at 15 min BstEII-cut R118C/D126C could already be cross-linked maximally and the fraction of monomeric 43-kD protein cross-linked remained relatively constant during the next 3 h as total translation increased. Similarly, the fraction of full-length protein cross-linked was already maximal as early as 15 min and constant as total translated protein continued to increase over the next 3 h. Regardless of whether attached intermediates or released full-length protein are used, the fraction of monomer chains cross-linked was maximal at 15 min and unchanged at 3 h. These results are consistent with T1−T1 association occurring in an oligomeric intermediate while the nascent chains are still attached to the ribosome.

DISCUSSION

Although the tetrameric crystal structure of the soluble T1 domain has been known since 1998 (*11*) and corroborated for several Kv proteins (*12*, *13*), the question remained as to whether this structure existed in full-length, mature Kv channels in the plasma membrane. Recent evidence shows that the T1 tetramer exists in the mature, full-length *Shaker* channel in the plasma membrane (*9*, *10*). We now provide direct evidence that folded T1 domains and T1−T1 interactions are already present in Kv1.3 tetramers in ER membranes. In addition, we demonstrate that folded T1 tetramers can form prior to polypeptide exit from the translocation channel, i.e., self-association of folded T1 domains occurs between ribosome-attached nascent subunits.

The amino acids involved in N-terminal self-association appear to be specific for residues at the T1−T1 interface. The initial contact between T1 domains may not be the same as the T1−T1 interface in the crystal structure or in the mature full-length channel in the plasma membrane. Nonetheless, some of the final interactions of the mature channel

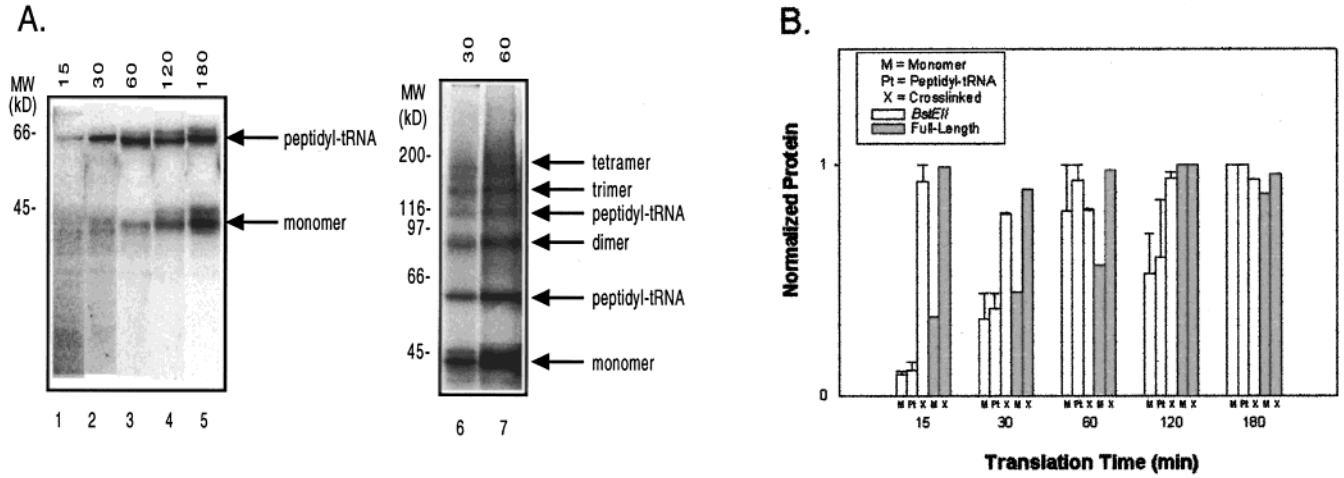

FIGURE 9: Cross-linking at various translation times. (A) *BstEII*-cut R118C/D126C was translated (lanes 1−5) for the times (min) indicated above each lane, then cross-linked (lanes 6 and 7) as described for Figure 4 and in Materials and Methods, and analyzed by LDS−NUPAGE (4−12% gels). (B) Fraction of protein cross-linked. Protein translated, peptidyl-tRNA, and fraction of monomeric 43-kD protein cross-linked were normalized at each time point to their respective maximal values and plotted as normalized values for the indicated translation times. Data were obtained by PhosphorImaging the Bis-Tris gels. For comparison, similar data (normalized translated protein and fraction of full-length protein cross-linked) from parallel samples of full-length R118C/D126C are shown. Data are the mean ± SEM for *BstEII*-cut R118C/D126C cross-linking at 15, 30, 60, and 120 min ($n = 3$) and the mean ± average deviation for *BstEII*-cut R118C/D126C translated protein and peptidyl-tRNA at 15, 30, 60, and 120 min ($n = 2$). The full-length data represent a single experiment.

are manifest at this early stage in biogenesis and require that the polypeptide chain fold while still bound to the ribosome. The membrane bilayer per se is not responsible for continuing to hold N-termini in close proximity. Nor are the ribosomes. Association persists even after the membrane and/or the ribosomes are removed from the complex, suggesting a direct, steadfast intrinsic interaction between amino acid side chains of the T1−T1 interface.

It appears that T1−T1 interaction occurs early in Kv1.3 biogenesis, although we cannot yet conclude that intersubunit T1 tetramerization occurs while the Kv1.3 chain is being elongated. Two recently described precedents exist in non-channel systems for polysomal cotranslational oligomerization, i.e., association that occurs while the nascent chains are being synthesized. The reovirus cell attachment protein forms polysome-associated trimers (26), and the Rel homology domain of NF-κB1, a mammalian protein, dimerizes co-translationally (27). In the latter case, a dimer forms between the adjacent ribosomes. Both examples are cytosolic proteins, which are generated in the cytoplasm and have no apparent alternative way to oligomerize efficiently using a confining structure such as the ER membrane. The linking polysome is the structure that holds the nascent chains in proximity and provides the initiation site for efficient oligomerization. Such mechanisms may also prevail for membrane-integrated homooligomers such as Kv channels, perhaps facilitating tetramer formation.

How close do nascent N-termini of Kv1.3 get to each other while attached to neighboring ribosomes? On the basis of *o*-PDM measurements, the N-termini approach each other within 6 Å. On the basis of multimer formation under oxidizing conditions, N-termini can even approach within 2 Å. The observed fraction of protein that can be cross-linked (≥50% for T1-specific engineered pairs of cysteines) precludes this proximity being a rare event. Moreover, general protein mobility cannot account for cross-linking as control constructs yield significantly lower amounts of cross-linked oligomers (Figure 5D). In the primary Kv1.3 sequence, 180 N-terminal amino acids precede the first transmembrane segment (S1) and appear to be exposed in the cytosol (*28*). A rendezvous of the engineered pairs from two adjacent unfolded chains would create a bridge of 120 amino acids for R118C/D126C and R116C/E130C. Although we do not know the secondary or tertiary structure of ribosome-attached T1, this number of intervening amino acids provides a maximum total distance of ∼400 Å if the protein were unfolded and maximally extended, assuming 3.4 Å/amino acid for an β-strand. Since these proteins are folded, ribosome/translocon complexes are likely ≪ 400 Å apart and may even be close enough to touch (*29*).

Does this T1−T1 association occur on the same polysome (intrapolysomal) or between polysomes (interpolysomal)? Our data clearly show that interpolysomal association occurs, but do not preclude intrapolysomal association. Kv1.x heterotetramers not only exist in mammalian brain (*30*−*35*) but can also constitute the major population of Kv1.x channels in specific regions of the brain (*34*). It is not clear whether this in vivo distribution is random or preferential (possibly regulated) assembly. On the other hand, heterologous expression (in oocytes or cultured cells) of two differently tagged Kv subunits of the same channel protein results in a binomial distribution of channel compositions (e.g., *36* and *37*) and suggests that the assembly of subunits is a random process. However, in these cases it is not clear at which stage of assembly the randomness occurs. We previously concluded that the four subunits in any given tetramer were not translated and preferentially assembled from the same polysome (*38*). This may only hold for heterologous expression, which is done, by definition, at high expression levels. In this case, the density of polysomes on ER membrane may be exceedingly high, and randomness could be at the polysome level. Hence, random (interpolysome) versus preferential (intrapolysome) distribution may be dependent on the relative ratios of two different mRNAs or on a specific regulator. Three lines of evidence favor this hypothesis. First, influenza hemagglutinin trimers in double-

infected cells are not randomly assembled into mixed trimers when expressed at low levels, in contrast to the results found at high expression levels (*39*, *40*). Second, expression of two different IP_3 receptor channel isoforms in COS cells yields both homo- and hetero-oligomers, the former being favored over the latter, and the lag time for synthesis of hetero-oligomers is greater than the lag time for synthesis of homotetramers (*41*). Third, several examples of nonrandom subunit composition or arrangement exist (*42*−*44*). In some studies where homooligomers may be preferred over heteromers, this could be due to a higher probability of successful oligomer formation per collision between like subunits.

It appears that membranes facilitate initial association of membrane-targeted proteins, a feature that could underlie efficient ER assembly of oligomeric complexes, in general (*45*), and of Kv channels, in particular (*17*). Three scenarios may be considered to account for membrane-facilitated cross-linking of the N-termini. First, interaction of nascent peptide with ER membrane protein translocating machinery (e.g., the translocon or lumenal enzymes and chaperones) may permit T1s to orient or fold correctly and/or restrict their motion in three dimensions. Second, integration of some, but not all, transmembrane segments into the bilayer could likewise serve to globally restrict subunits and promote T1−T1 interactions. Third, the cytosolic NH_2-terminus could adsorb onto the lipid surface and thereby be restricted to the plane of the bilayer. In each case, the consequence would be to concentrate T1 domains and catalyze T1 tetramerization.

The results showing membrane-facilitated T1−T1 association, and no evidence for cross-linking of nascent peptides on free polysomes, are provocative in view of the fact that T1 tetramers form in solution when just the T1 peptide itself is made (*3*, *11*, *13*, *46*−*48*). In these cases, the peptide is released into aqueous solution and can freely associate and dissociate. However, when T1 is tethered to the rest of the Kv protein being synthesized on the ribosome, it may be constrained or not available to oligomerize until it is targeted to the membrane. Chaperone factors, and even the ribosome itself, could decrease T1 accessibility and prevent untimely oligomerization. In previous studies, we have demonstrated that although S1 has signal sequence activity and by itself can target to the ER membrane, S1 attached to the complete cytosolic N-terminus does not (*28*).[3] If the N-terminus plus S1 forms a folded structure that inhibits signal sequence activity, then stable folding of N-terminal domains of integrated membrane proteins may not only hinder N-terminal translocation (*49*), but may also protect against premature oligomerization before the channel protein reaches the ER membrane. Events at the translocon may refold the N-terminus or allosterically induce an oligomeric-competent T1. Precedents in nonchannel proteins exist (*50*).

We have previously proposed that T1−T1 interaction may serve to globally restrict nascent peptide chains of individual subunits (*28*, *51*). Similarly, Zerangue et al. have proposed that T1-tetramerization promotes a high concentration of monomers for speedy tetramerization of the transmembrane parts of the channel (*52*). Our results confirm these hypotheses, demonstrating that T1-linked tetramers, but no higher order oligomers, form on membrane-associated ribosomes prior to polypeptide exit from the translocon. The precise temporal relationship between T1−T1 association and integration of the peptide into the bilayer awaits further elucidation as some part, but not all, of the polypeptide could have integrated while translation continued. Nonetheless, T1−T1 interaction may be the first and earliest event in channel assembly, occurring during translation and perhaps even before membrane integration. Whether this occurs in vivo remains to be shown. In addition to T1 interactions, however, there must be other mechanisms for effecting tetramer formation, as T1-deleted Kv1.3 subunits can eventually associate via transmembrane domains (*20*) to form stable, functional channels. In this case, both the rates and efficiency of tetramer formation are significantly lower (*20*, *53*), which is clearly manifest in sucrose gradient measurements (*16*) and electrophysiological studies (*20*). High concentrations of T1-deleted constructs are necessary to effect functional expression (*20*, *54*). This is consistent with the interpretation that T1−T1 association precedes and facilitates intersubunit transmembrane tetramerization, rather than the reverse sequence of events. We suggest that early T1−T1 interactions of ribosome-attached nascent chains kinetically expedite oligomerization, bringing nascent subunits into proximity, but T1−T1 interactions may not provide all, or even the major, stabilization energy that is responsible for tetramerization in full-length Kv channels.

[3] S2 likely functions as the initial signal sequence in Kv1.3 (*28*).

ACKNOWLEDGMENT

We thank Dr. C. Nicchitta for extensive advice and discussion in the course of this work and for critical reading of the manuscript. We thank Dr. R. Horn for his critical reading of the manuscript. We thank Dr. L. Tu and J. Wang for contributing the oocyte experiments.

REFERENCES

1. Rosenberg, R. L., and East, J. E. (1992) *Nature 360*, 166−169.
2. Li, M., Jan, Y. N., and Jan, L. Y. (1992) *Science 257*, 1225−1230.
3. Shen, N. V., Chen, X., Boyer, M. M., and Pfaffinger, P. (1993) *Neuron 11*, 67−76.
4. Deal, K. K., Lovinger, D. M., and Tamkun, M. M. (1994) *J. Neurosci. 14*, 1666−1676.
5. Nagaya, N. and Papazian, D. M. (1997) *J. Biol. Chem. 272*, 3022−3027.
6. Sewing, S., Roeper, J., and Pongs, O. (1996) *Neuron 16*, 455−463.
7. Yu, W., Xu, J., and Li, M. (1996) *Neuron 16*, 441−453.
8. Schulteis, C. T., Nagaya, N., and Papazian, D. M. (1998) *J. Biol. Chem. 273*, 26210−26217.
9. Kobertz, W. R., Williams, C., and Miller, C. (2000) *Biochemistry 39*, 10347−10352.
10. Sokolova, O., Kolmakova-Partensky, L., and Grigorieff, N. (2001) *Structure 9*, 215−220.
11. Kreusch, A., Pfaffinger, P. J., Stevens, C. F., and Choe, S. (1998) *Nature 392*, 945−948.
12. Bixby, K. A., Nanao, M. H., Shen, N. V., Kreusch, A., Bellamy, H., Pfaffinger, P. J., and Choe, S. (1999) *Nat. Struct. Biol. 6*, 38−43.
13. Minor, D. L., Lin, Y. F., Mobley, B. C., Avelar, A., Jan, Y. N., Jan, L. Y., and Berger, J. M. (2000) *Cell 102*, 657−670.
14. Chahine, M., Chen, L.-Q., Barchi, R. L., Kallen, R. G., and Horn, R. (1992) *J. Mol. Cell Cardiol. 24*, 1231−1236.
15. Lu, J., and Deutsch, C. (2001) *Biochemistry* (in press).

16. Lu, J., and Deutsch, C. (1999) *Biophys. J. 76*, A76.
17. Sheng, Z., Skach, W., Santarelli, V., and Deutsch, C. (1997) *Biochemistry 36*, 15501−15513.
18. Wu, J., and Kaback, H. R. (1997) *J. Mol. Biol. 270*, 285−293.
19. Marquardt, T., Hebert, D. N., and Helenius, A. (1993) *J. Biol. Chem. 268*, 19618−19625.
20. Tu, L., Santarelli, V., Sheng, Z.-F., Skach, W., Pain, D., and Deutsch, C. (1996) *J. Biol. Chem. 271*, 18904−18911.
21. Sheng, Z., Skach, W., Santarelli, V., and Deutsch, C. (1997) *Biochemistry 36*, 15501−15513.
22. Traut, R. R. and Monro, R. E. (1964) *J. Mol. Biol. 10*, 63−72.
23. Monro, R. E., Staehelin, T., Celma, M. L., and Vazquez, D. (1969) *Cold Spring Harbor Symposia on Quantitative Biology 34*, 357−368.
24. Gilmore, R., Collins, P., Johnson, J., Kellaris, K., and Rapiejko, P. (1991) *Methods Cell Biol. 34*, 223−239.
25. Matlack, K. E. and Walter, P. (1995) *J. Biol. Chem. 270*, 6170−6180.
26. Gilmore, R., Coffey, M. C., Leone, G., McLure, K., and Lee, P. W. (1996) *EMBO J. 15*, 2651−2658.
27. Lin, L., DeMartino, G. N., and Greene, W. C. (2000) *EMBO J. 19*, 4712−4722.
28. Tu, L., Wang, J., Helm, A., Skach, W. R., and Deutsch, C. (2000) *Biochemistry 39*, 824−836.
29. Wolin, S. L. and Walter, P. (1988) *EMBO J. 7*, 3559−3569.
30. Wang, H., Kunkel, D. D., Martin, T. M., Schwartzkroin, P. A., and Tempel, B. L. (1993) *Nature 365*, 75−79.
31. Sheng, M., Liao, Y. L., Jan, Y. N., and Jan, L. Y. (1993) *Nature 365*, 72−75.
32. Scott, V. E., Muniz, Z. M., Sewing, S., Lichtinghagen, R., Parcej, D. N., Pongs, O., and Dolly, J. O. (1994) *Biochemistry 33*, 1617−1623.
33. Veh, R. W., Lichtinghagen, R., Sewing, S., Wunder, F., Grumbach, I. M., and Pongs, O. (1995) *Eur. J. Neurosci. 7*, 2189−2205.
34. Koch, R. O., Wanner, S. G., Koschak, A., Hanner, M., Schwarzer, C., Kaczorowski, G. J., Slaughter, R. S., Garcia, M. L., and Knaus, H. G. (1997) *J. Biol. Chem. 272*, 27577−27581.
35. Shamotienko, O. G., Parcej, D. N., and Dolly, J. O. (1997) *Biochemistry 36*, 8195−8201.
36. MacKinnon, R. (1991) *Nature 350*, 232−235.
37. Panyi, G., Sheng, Z., Tu, L., and Deutsch, C. (1995) *Biophys. J. 69*, 896−904.
38. Panyi, G., and Deutsch, C. (1996) *J. General Physiol. 107*, 409−420.
39. Hurtley, S. M., and Helenius, A. (1989) *Annu. Rev. Cell Biol. 5*, 277−307.
40. Boulay, F., Doms, R. W., Webster, R. G., and Helenius, A. (1988) *J. Cell Biol. 106*, 629−639.
41. Joseph, S. K., Bokkala, S., Boehning, D., and Zeigler, S. (2000) *J. Biol. Chem. 275*, 16084−16090.
42. Glowatzki, E., Fakler, G., Brandle, U., Rexhausen, U., Zenner, H. P., Ruppersberg, J. P., and Fakler, B. (1995) *Proc. Royal Soc. London - Ser. B: Biol. Sci. 261*, 251−261.
43. Pessia, M., Tucker, S. J., Lee, K., Bond, C. T., and Adelman, J. P. (1996) *EMBO J. 15*, 2980−2987.
44. Corey, S., Krapivinsky, G., Krapivinsky, L., and Clapham, D. E. (1998) *J. Biol. Chem. 273*, 5271−5278.
45. Helenius, A., Marquardt, T., and Braakman, I. (1992) *Trends Cell Biol. 2*, 227−231.
46. Li, M., Jan, Y. N., and Jan, L. Y. (1992) *Science 257*, 1225−1230.
47. Babila, T., Moscucci, A., Wang, H., Weaver, F. E., and Koren, G. (1994) *Neuron 12*, 615−626.
48. Pfaffinger, P. J., and DeRubeis, D. (1995) *J. Biol. Chem. 270*, 28595−28600.
49. Denzer, A. J., Nabholz, C. E., and Spiess, M. (1995) *EMBO J. 14*, 6311−6317.
50. Schatz, G., and Dobberstein, B. (1996) *Science 271*, 1519−1526.
51. Tu, L., and Deutsch, C. (1999) *Biophys. J. 76*, 2004−2017.
52. Zerangue, N., Jan, Y. N., and Jan, L. Y. (2000) *Proc. Nat. Acad. Sci. U.S.A. 97*, 3591−3595.
53. Tu., L., Santarelli, V., and Deutsch, C. (1995) *Biophys. J. 68*, 147−156.
54. Kobertz, W. R. and Miller, C. (1999) *Nat. Struct. Biol. 6*, 1122−1125.
55. Tu, L. and Deutsch, C. (1999) *Biophys. J. 76*, 2004−2017.

BI010763E